Journal of Cellular Biochemistry 94:585–596 (2005)

Deregulation of DNA Methyltransferases and Loss of Parental Methylation at the Insulin-Like Growth Factor II (*Igf2*)/*H19* Loci in *p53* Knockout Mice Prior to Tumor Development

In Young Park,[1] Bo Hwa Sohn,[2] Jung Ha Choo,[1] Cheol O. Joe,[1] Je Kyung Seong,[3] Young Ik Lee,[2] and Jae Hoon Chung[1]*

[1]Department of Biological Sciences, Korea Advanced Institute of Science and Technology, Taejon 305-701, Republic of Korea
[2]Laboratory of Liver Cell Signal Transduction, Korea Research Institute of Bioscience and Biotechnology, Taejon 305-333, Republic of Korea
[3]Laboratory of Developmental Biology and Genomics, College of Veterinary Medicine, Seoul National University, Seoul 151-742, Republic of Korea

Abstract To ascertain whether *p53* deficiency in vivo leads to the deregulation of DNA methylation machinery prior to tumor development, we investigated the expression profile of DNA methyltransferases in the thymus and the liver of $p53^{+/+}$, $p53^{+/-}$, and $p53^{-/-}$ mice at 7 weeks of age before tumor development. The expression of DNA methyltransferases was examined in the thymus at 7 weeks of age, since the malignant T-cell lymphoma develops most frequently in $p53^{-/-}$ mice around 20 weeks of age. Both mRNA and protein levels of *Dnmt1* and *Dnmt3b* were increased in the thymus and the liver of *p53*-deficient mice. The expression of *Dnmt3a* was also increased in the liver but not in the thymus of *p53*-deficient mice. *Dnmt3L* expression was reduced in the thymus of $p53^{+/-}$ and $p53^{-/-}$ mice. The total 5-methylcytosine (5-MeC) in the genomic DNA of $p53^{+/+}$, $p53^{+/-}$, and $p53^{-/-}$ mice was quantitated by dot-blot using antibody against 5-MeC. Global methylation was increased in the thymus and the liver of *p53*-deficient mice. To correlate the deregulated expression of DNA methyltransferases with the disturbance of the epigenetic integrity, we examined the DNA methylation of the imprinting control region (ICR) at the insulin-like growth factor II (*Igf2*)/*H19* loci in the thymus and the liver of $p53^{+/+}$, $p53^{+/-}$, and $p53^{-/-}$ mice. The region containing two CCCTC binding factor (CTCF) binding sites in the 5′-ICR tended to be hypomethylated in the thymus of $p53^{-/-}$ mice, but not in the liver. The expression profile of *Igf2* and *H19* indicated that the thymus-specific changes of *Igf2* and *H19* expression were coherent to the hypomethylation of the ICR in the thymus. Our results suggest that p53 is required for the maintenance of DNA methylation patterns in vivo. J. Cell. Biochem. 94: 585–596, 2005.

Key words: *p53*; DNA methyltransferase; insulin-like growth factor 2 (*Igf2*); *H19*; imprinting control region (ICR); DNA methylation

Regional hypermethylation of several tumor suppressor genes despite genome-wide hypomethylation is one of the representative epigenetic modifications in cancers [Jones and Baylin, 2002]. Contrary to the genomic hypomethylation, DNA methyltransferases are usually overexpressed in cancers [Robertson et al., 1999]. The deregulated DNA methyltransferases found in tumors are DNA methyltransferase 1 (Dnmt1), a maintenance enzyme, Dnmt3a and Dnmt3b, de novo DNA methyltransferases [Robertson et al., 1999]. However, the expression of Dnmt3L, known to be essential for the establishment of maternal DNA methylation imprints [Bourc'his et al., 2001; Hata et al., 2002], has not been reported in

Grant sponsor: Ministry of Science and Technology (Molecular and Cellular Biodiscovery Research Group Program); Grant number: M1-0106-04-0001.

*Correspondence to: Jae Hoon Chung, PhD, Department of Biological Sciences, 373-1 Gusung-Dong, Yusung-Gu, Korea Advanced Institute of Science and Technology, Taejon 305-701, Republic of Korea. E-mail: jhc@kaist.ac.kr

Received 18 December 2003; Accepted 14 June 2004

DOI 10.1002/jcb.20263

tumors. Although the genomic DNA methylation changes in various tumors have been extensively investigated, the epigenetic studies on Li–Fraumeni syndrome have been rarely reported. Li–Fraumeni syndrome is caused by germline transmission of *TP53* mutant allele [Srivastava et al., 1990]. The $p53^{-/-}$ mice, a mouse model of Li–Fraumeni syndrome, developed the malignant T-cell lymphoma at 3–6 months of age [Donehower et al., 1992; Jacks et al., 1994]. Using $p53^{-/-}$ mice before tumor development, the in vivo role of p53 in DNA methylation homeostasis could be elucidated. The deregulation of DNA methyltransferases would be expected in the thymus of *p53* knockout mice before tumor development if the depletion of p53 resulted in the abnormal DNA methylation

Insulin-like growth factor 2 (*Igf2*) is a maternally imprinted gene linked to the paternally imprinted *H19* on the mouse chromosome 7, being expressed exclusively from the hypermethylated paternal allele of *Igf2* [Ferguson-Smith et al., 1991]. The control sites for the imprinted expression are located at differentially methylated region (DMR) 1 on *Igf2* promoter, DMR2 on exon 4–6 of *Igf2*, and imprinting control region (ICR) at 2 kb upstream of *H19* [Vu and Hoffman, 1994; Hark et al., 2000]. The differential DNA methylation pattern of the ICR is allelically most distinctive among the DMRs of the imprinted regions known to date [Weber et al., 2001]. The maternally unmethylated ICR acts as a boundary/insulator element mediated by a zinc finger protein CCCTC binding factor (CTCF) [Bell and Felsenfeld, 2000]. Hypermethylation on the maternal allele of the ICR is coincident with an increased expression of *IGF2* in Wilm's tumor [Cui et al., 2001]. The aberrant DNA methylation of the maternal ICR abolishes the CTCF binding. Loss of imprinting (LOI) is also found in colorectal, liver, lung cancers, and in leukemia [Hashimoto et al., 1995; Hibi et al., 1996; Takeda et al., 1996]. Hypomethylation on the paternal allele of the ICR has been also observed in colorectal cancer [Cui et al., 2002, 2003]. Both gain-of-methylation and loss-of-methylation on the ICR of the *IGF2*/*H19* loci occur in a mutually exclusive manner in osteosarcoma [Ulaner et al., 2003]. The methylation of the maternal allele accompanies *IGF2* LOI, while the demethylation of the paternal allele accompanies *H19* LOI in osteosarcoma [Ulaner et al., 2003]. Thus, the ICR of the *Igf2*/*H19* loci seems to contain the preferential target sequences for the aberrant DNA methylation in most tumors.

To demonstrate the disruption of epigenetic regulation by *p53* deficiency, the expression profiles of the DNA methylation machinery under varying degree of *p53* dosage were investigated using 7-week-old *p53*-deficient mice before tumor development. DNA methylation status of the ICR on the *Igf2*/*H19* loci was also investigated in the thymus of *p53*-deficient mice.

MATERIALS AND METHODS

Isolation of Total RNA and Genomic DNA From Thymus and Liver Specimens

Mice deficient in *p53* were obtained from The Jackson Laboratory, Bar Harbor, ME and maintained as heterozygotes under C57BL/6J background. Approximately 40% of the coding region of *p53* is removed in the *p53* mutant mice [Jacks et al., 1994]. Homozygotes were produced by mating male and female heterozygotes. Genotyping was performed as described [Jacks et al., 1994]. All the mice at 7 weeks of age without any apparent tumors were sacrificed. Liver and thymus were collected from $p53^{+/+}$, $p53^{+/-}$, and $p53^{-/-}$ mice. Butterfly-form thymus was incised between upper rib and heart. Genomic DNAs were isolated by standard procedures [Maniatis et al., 1982]. Total RNAs were extracted with TRIzol solution (Invitrogen, Carlsbad, CA) according to the manufacturer's specifications.

Quantitative RT-PCR Analysis

The expression levels of DNA methyltransferases, *Igf2*, and *H19* were quantitated by a real-time RT-PCR with LightCycler (Roche Applied Science, Mannheim, Germany). Total RNAs (15 μg) were reverse-transcribed in a volume of 100 μl by using First-Strand cDNA Synthesis Kit (Amersham Pharmacia Biotech, Seoul, South Korea). One microliter of synthesized cDNA was used for the analysis. Each reaction was performed in a 20 μl volume using the LightCycler DNA Master SYBR Green I (Roche Applied Science) in a thin-walled capillary tube. The conditions were programmed as follows: initial denaturation at 95°C for 10 s followed by 35 cycles of 5 s at 95°C, 10 s at

60°C, and 15 s at 72°C. Primers used in the quantitative RT-PCR are listed in Table I. The relative amounts of the mRNAs were determined using the Quantification program (Roche Applied Science). The amount of the PCR products was normalized to the percentage of the expression level of *β-Actin*. The RT-PCR products were also evaluated on 1.5% agarose gels after staining with ethidium bromide to ascertain the specificity of the experiments. The cycle numbers of the PCR were reduced in order to optimize the changes of band intensities. The numbers of cycles for the amplification of *β-Actin*, *p53*, *Dnmt1*, and *Dnmt3a* were 22, 25, 30, and 32, respectively. The rests of the PCR were performed for 35 cycles.

Immunoblot of DNA Methyltranferases

The tissue samples were homogenized in 1 ml of boiling lysis buffer (1% SDS, 1 mM sodium ortho-vanadate, 10 mM Tris, pH 7.4) using tissue-tearor (Biospec Products, Inc., Bartlesville, OK) and boiled briefly at 100°C for 10 s. The tissue lysates were centrifuged 13,000*g*, for 5 min and the protein concentrations were measured by Bio-Rad protein assay reagent (Bio-Rad Laboratories, Inc., Hercules, CA). The tissue lysates (15 μg) were eletrophoresed on SDS–PAGE gel (6% for Dnmt1 and 7.5% for Dnmt3a, 3b, 3L, α-Tubulin). The electrotransferred membranes were probed with a 1: 2,000 dilution of anti-Dnmt1 antibody (Imgenex, San Diego, CA), anti-Dnmt3a antibody (Imgenex), anti-Dnmt3b antibody (Abgent, San Diego, CA), anti-Dnmt3L antibody (Abgent), anti-p53 antibody (Santa Cruz Biotechnology, Inc., Santa Cruz, CA), or anti-α-Tubulin antibody (Oncogene Research Products, San Diego, CA). HRP-conjugated anti-mouse IgG antibody (Santa Cruz Biotechnology, Inc.) was used as a secondary antibody for Dnmt1, Dnmt3a, and α-Tubulin, while anti-rabbit IgG antibody (Santa Cruz Biotechnology, Inc.) for Dnmt3b, Dnmt3L, and p53.

5-Methylcytosine (5-Mec) Dot-Blot Analysis With the Genomic DNA

Dot-blot analysis using antibody against 5-MeC was performed as described [Tao et al., 2004]. Genomic DNA (2 μg) was denatured by adding NaOH and EDTA solution to final concentration of 0.4 N NaOH, 10 mM EDTA and heated to 100°C for 10 min. The DNA samples were neutralized by adding an equal volume of cold 2 M ammonium acetate, pH 7.0 and then dotted onto a Hybond™-ECL™ nitrocellulose membrane (Amersham Pharmacia Biotech) using a Bio-Dot Microfiltration Apparatus (Bio-Rad Laboratories, Inc.). The membrane was crosslinked in Ultraviolet crosslinker (Amersham Pharmacia Biotech) for 2 min and incubated in a 5% skim milk/Tris-buffered saline + Tween 20 (TBST) blocking solution (pH 7.5) for 2 h. The membrane was probed with a 1: 2,000 dilution of sheep polyclonal primary antibody (Abcam, Cambridgeshire, UK) specific against 5-MeC for 2 h, washed three times for 15 min with TBST (pH 7.5), and incubated with 1:2,000 dilution of (HRP)-conjugated secondary anti-sheep IgG antibody for 1 h. The membrane was washed again with TBST, treated with ECL plus Western blotting detection reagent (Amersham Parmacia Biotech) and autoradiographed. The equal quantiy of the genomic DNA was indicated by the

TABLE I. Primers Used in Quantitative RT-PCR

Gene	Orientation	Sequence
β-Actin	Sense	5′-GGTTCCGATGCCCTGAGGCTCTTT-3′
	Antisense	5′-CGCAGCTCAGTAACAGTCCGCCTA-3′
Igf2	Sense	5′-TGTTCGGACCGCGGCTTCTACTTC-3′
	Antisense	5′-ACACGATCAGGGGACGATGACGTTTG-3′
H19	Sense	5′-TGATCGGTGTCTCGAAGAGCTCGG-3′
	Antisense	5′-TGACACCATCTGTTCTTTCAGCTTCAC-3′
Dnmt1	Sense	5′-CCAAGCTCCGGACCCTGGATGTGT-3′
	Antisense	5′-CGAGGCCGGTAGTAGTCACAGTAG-3′
Dnmt3a	Sense	5′-GCACCTATGGGCTGCTGCGAAGACG-3′
	Antisense	5′-CTGCCTCCAATCACCAGGTCGAATG-3′
Dnmt3b	Sense	5′-CAAGGAGGGCGACAACCGTCCATT-3′
	Antisense	5′-TGTTGGACACGTCCGTGTAGTGAG-3′
Dnmt3L	Sense	5′-CCCTAGGCAGCTCTTGTGATCGCTG-3′
	Antisense	5′-CGTCCAGCTTGCTCCTGCTTCTGAC-3′

intensity of 0.02% methylene blue staining. The relative dot intensity was measured using GS-800^{TM} calibrated densitometer (Bio-Rad Laboratories, Inc.).

Combined Bisulfite Restriction Analysis (COBRA) and Bisulfite Sequencing

Bisulfite treatment and COBRA were performed as described [Xiong and Laird, 1997]. One microgram of the genomic DNA of each sample was denatured in 0.2 M NaOH. Sodium bisulfite (Sigma, St. Louis, MO) was added to a final concentration of 3.1 M, and hydroquinone to a final concentration of 0.5 mM. The reaction was performed at 55°C for 16 h. The DNA samples were purified with the DNA Clean-Up System (Promega, Madison, WI) and then desulfonated by 0.3 M NaOH and precipitated with ethanol. Ten nanograms of the modified DNA was amplified in 5% DMSO, 20 mM Tris-HCl pH 8.8, 2 mM $MgCl_2$, 10 mM KCl, 1.25 mM dNTPs, 400 nM of primer pairs, and 5 U Taq DNA polymerase (Roche Applied Science). Cycling conditions were at 94°C for 5 min followed by 40 cycles of 94°C for 30 s, 55°C for 30 s, and 72°C for 2 min with a final extension of 5 min at 72°C. The PCR products were purified using QIAquick PCR Purification Kit (Qiagen, Valencia, CA). The full bisulfite conversion was confirmed by digestion with KpnI (New England Biolabs, Beverly, MA) for the ICR of *Igf2*/*H19*, or HhaI (New England Biolabs) for *Peg1* and *Peg3*, since KpnI or HhaI cleaves the unconverted DNA sequence. The PCR products uncleavable by KpnI or HhaI were used for COBRA. The fully converted PCR products was digested with ClaI (New England Biolabs) for the ICR of *Igf2*/*H19*, RsaI (Roche Applied Science) for *Peg1*, or TaqI (Roche Applied Science) for *Peg3*, and electrophoresed on a 2% agarose gel. The fully converted PCR products of the ICR were also cloned using pGEM-T-easy vector system (Promega) for DNA sequencing analysis. Primer sequences for the PCR amplification of the ICR at the *Igf2*/*H19* loci were: 5′-GAGTATTTAGGAGGTATAAGA-3′ (sense, upper strand) and 5′-CAAAAACTAACATAAACCCCT-3′ (antisense, upper strand).

RESULTS

Altered Expression of DNA Methyltransferases in *p53*-Deficient Mice

To determine whether the regulation of DNA methylation machinery is affected by *p53* deficiency before tumor development, we tested the expression of DNA methyltransferases in the thymus and the liver of $p53^{+/+}$, $p53^{+/-}$, and $p53^{-/-}$ mice at 7 weeks of age. The thymus was chosen to detect the abnormal expression of DNA methyltransferases since most tumors developed in $p53^{-/-}$ mice at 20 weeks of age were mostly thymic lymphomas [Donehower et al., 1992; Harvey et al., 1993]. Liver was also investigated as a control. No tumors were detected in all the tissues of the mice sacrificed. The mRNA levels of *Dnmt1* and *Dnmt3b* were increased in the thymus and in the liver of *p53*-deficient mice (Fig. 1A,B). The increments of *Dnmt1* transcripts relative to wild type mice were 9.3 and 34.1% in the thymus of $p53^{+/-}$ and $p53^{-/-}$ mice, respectively (Fig. 1A,B). The increased expression of *Dnmt1* was prominent in the liver. Its increased quantities relative to wild type mice were 27.8 and 101.5% in the liver of $p53^{+/-}$ and $p53^{-/-}$ mice, respectively. The increased mRNA levels of *Dnmt3b* relative to wild type mice were 77.8 and 55.4% in the thymus of $p53^{+/-}$ and $p53^{-/-}$ mice, and 56.6 and 50.7% in the liver of $p53^{+/-}$ and $p53^{-/-}$ mice, respectively. No specific isoform prevailed among the alternative splicing forms of *Dnmt3b*. The *Dnmt3a* expression did not vary significantly in the thymus, while 37.8 and 84.9% increases relative to wild type mice were observed in the liver of $p53^{+/-}$ and $p53^{-/-}$ mice, respectively. The expression of *Dnmt3L* was severely diminished in the thymus of $p53^{+/-}$ and $p53^{-/-}$ mice while no *Dnmt3L* transcript was detected in the liver irrespective of the *p53* genotypes. Protein

Fig. 1. The expression profiles of the DNA methyltransferases. **A**: Ethidium bromide staining of RT-PCR products of *Dnmt1*, *Dnmt3a*, *Dnmt3b*, and *Dnmt3L* transcripts. The RT-PCR cycle numbers of *Dnmt1*, *Dnmt3a*, *Dnmt3b*, *p53*, and *β-Actin* were 30, 32, 35, 25 and 22, respectively. The alternative splicing forms of *Dnmt3b* were designated with arrow. The RT-PCR products from the thymus and the liver of wild type mice and *p53*-deficient mice were shown. RT (+) and RT (−) PCR with *β-Actin* primers was used as a control. **B**: Quantitative real-time RT-PCR. The expression levels of DNA methyltransferases were also quantitated by real-time RT-PCR with LightCycler using SYBR Green I dye. The relative amounts of the mRNAs were analyzed using Quantification program and normalized as percentage against the expression level of the control *β-Actin*. **C**: Immunoblot of DNA methyltransferases. The equalized protein quantities were displayed by α-Tubulin as a control.

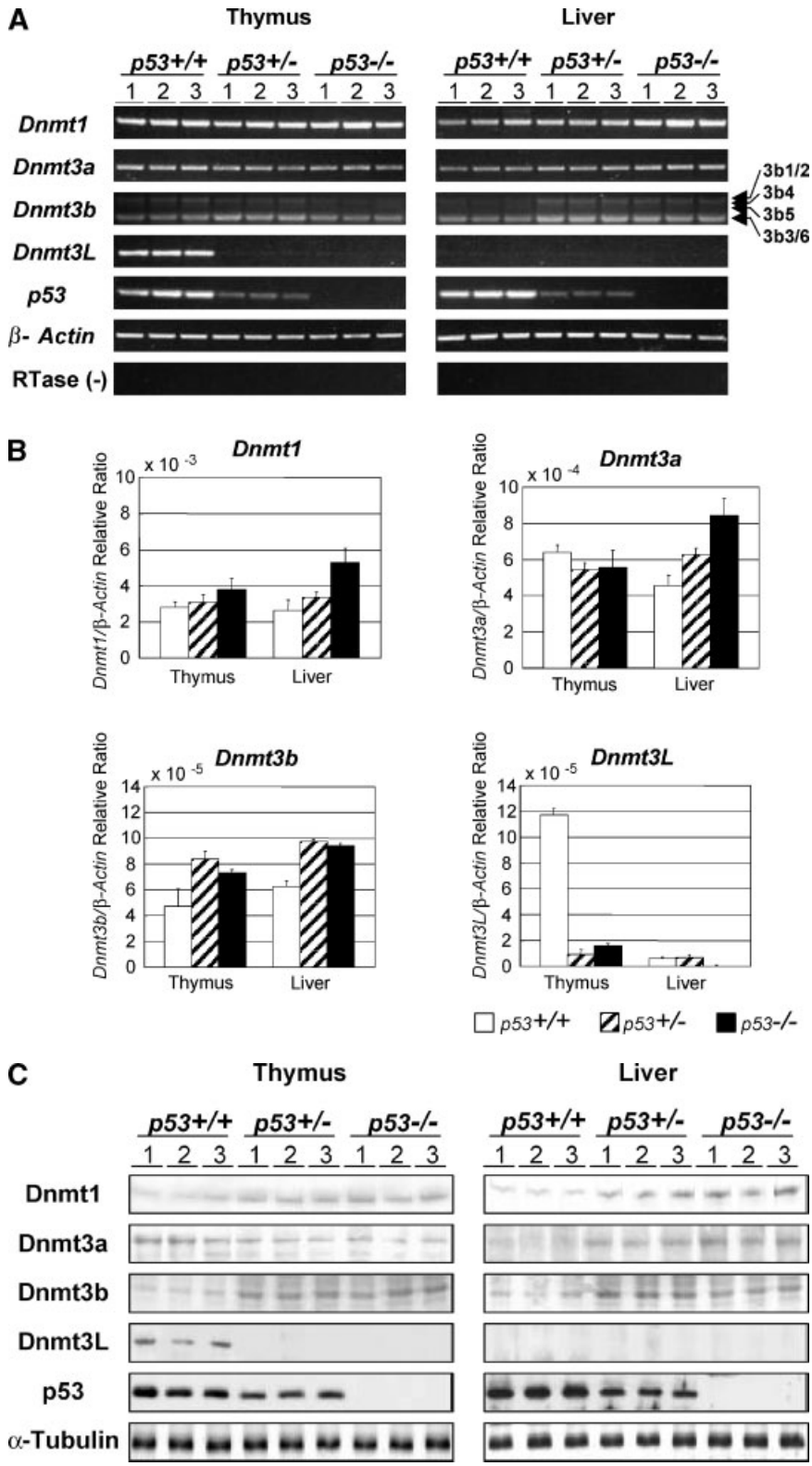
A
Thymus
Liver
p53+/+
p53+/-
p53-/-
1 2 3 1 2 3 1 2 3
Dnmt1
Dnmt3a
Dnmt3b
Dnmt3L
p53
β- Actin
RTase (-)
3b1/2
3b4
3b5
3b3/6
B
Dnmt1
Dnmt3a
Dnmt3b
Dnmt3L
Dnmt1/β-Actin Relative Ratio
Dnmt3a/β-Actin Relative Ratio
Dnmt3b/β-Actin Relative Ratio
Dnmt3L/β-Actin Relative Ratio
x 10 -3
x 10 -4
x 10 -5
Thymus
Liver
p53+/+
p53+/-
p53-/-
C
Thymus
Liver
Dnmt1
Dnmt3a
Dnmt3b
Dnmt3L
p53
α-Tubulin

Fig. 1.

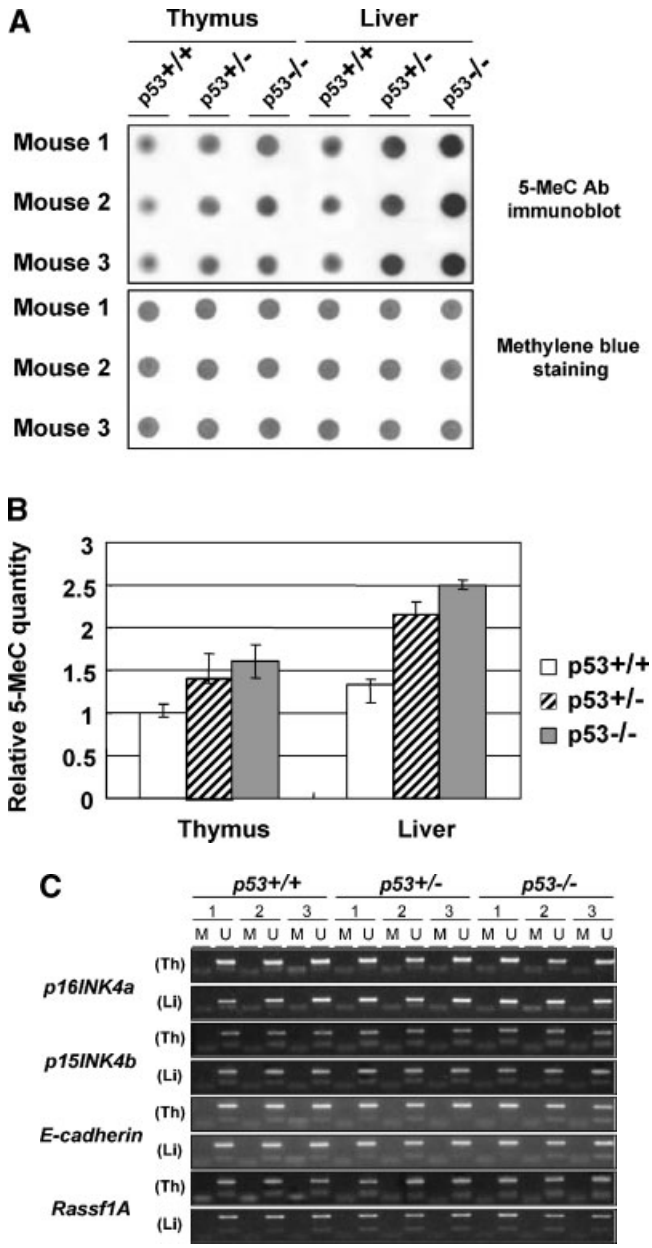

Fig. 2. Genomic 5-methylcytosine (5-MeC) contents and DNA methylation of tumor suppressor genes. **A**: The dot-blot analysis of 5-MeC in the thymus and the liver DNA. Genomic DNA (2 μg) was dot-blotted, bound by anti-5-MeC antibody, and detected chemiluminescence Western blot detection reagents. Equal loading was confirmed by 0.02% methylene blue staining. **B**: Comparative 5-MeC quantities in the thymus and the liver depending on *p53*-gene dosage. Statistical significance was determined by *t*-test with Bonferroni correction (*P*-value <0.05). **C**: MSP of *p16INK4a*, *p15INK4b*, *E-cadherin*, and *Rassf1A*. No methyl-specific bands were detected. The PCR conditions were the same for COBRA except annealing temperatures, 58°C. The primers used in COBRA and MSP were designated in Table II.

levels of all the DNA methyltransferases were approximately proportional to their mRNA levels (Fig. 1C). Thus, both transcriptional and translational levels of DNA methyltransferases were changed in *p53*-deficient mice before tumor develpment.

Global Hypermethylation in *p53*-Deficient Mice

The total genomic 5-MeC contents were measured by 5-MeC dot-blot to emphasize the consequence of the deregulated expression of the DNA methyltransferases. The genomic

TABLE II. Primers Used in COBRA or MSP

Gene	GenBank no.	Orientation	Sequences
Peg1	AF017994	Sense	5′-GGTGTTGGTATTTTTAGTGTTA-3′
		Antisense	5′-AAAAATCATCTTTCACACCTTC-3′
Peg3	AF105262	Sense	5′-GTAGAGGATTTTGATAAGGAG-3′
		Antisense	5′-CAATCTACAACCTTATCAATTA-3′
p161NK4a (methylated)	NT_039271	Sense	5′-G**CG**GTAGGGTT**CGCGC**-3′
		Antisense	5′-**CG**AAACCCA**CGCG**C**CG**-3′
p161NK4a (unmethylated)		Sense	5′-GATG**TG**GTAGGGTT**TGTGT**-3′
		Antisense	5′-CCT**CA**AAACCCA**CACA**C**CA**-3′
p151NK4b (methylated)	NT_039271	Sense	5′-GG**CG**TTAG**CG**TT**CG**AGC-3′
		Antisense	5′-**GCG**C**CGCG**A**CG**ATAAC-3′
p151NK4b (unmethylated)		Sense	5′-TAGG**TG**TTAG**TG**TT**TG**AG**TG**-3′
		Antisense	5′-C**ACA**C**CACA**A**CA**ATAACCA-3′
E-cadherin (methylated)	NT_078586	Sense	5′-GTTAGGATT**CG**AA**CG**AT**C**-3′
		Antisense	5′-ACTCAATAATA**CG**C**CGCG**-3′
E-cadherin (unmethylated)		Sense	5′-GGTTAGGATT**TG**AA**TG**AT**TG**-3′
		Antisense	5′-ACTCAATAATA**CA**C**CACA**AC-3′
Rassf1A (methylated)	NT_039477	Sense	5′-G**CG**TATA**CG**TTT**CG**GTT**C**-3′
		Antisense	5′-**CG**C**CGCGCG**ACAAC**CG**-3′
Rassf1A (unmethylated)		Sense	5′-ATG**TG**TATA**TG**TTT**TG**GTT**TG**-3′
		Antisense	5′-CAA**CA**C**CACACA**ACAAC**CA**-3′

CpG sites of MSP were indicated as underlined with bold letter.

5-MeC increased in the thymus and the liver as the *p53* gene dosage decrease. The increased quantities were 40.3% ($p53^{+/-}$), 60.3% ($p53^{-/-}$) in the thymus, and 62.7% ($p53^{+/-}$), 88.9% ($p53^{-/-}$) in the liver of $p53^{+/-}$ and $p53^{-/-}$ mice, respectively (Fig. 2A,B). The increase of the global genomic CpG methylation was prominent in the liver of *p53*-deficient mice. The high 5-MeC quantities in *p53*-deficient mice correlated with the increased expression of *Dnmt1* and *Dnmt3b*, while the reduced *Dnmt3L* expression barely influenced to the global genomic methylation pattern.

To ascertain whether the frequent tumor development in *p53*-deficient mice is due to the hypermethylation of tumor suppressor genes, DNA methylation of the representative tumor suppressor genes, *p16INK4a*, *p15INK4b*, *E-cadherin*, and *Rassf1A* was investigated by methylation-specific PCR (MSP). MSP primers were designed to amplify the region including the CpG islands at the promoter of the tumor suppressor genes (Table II). No methylation was detected in these tumor suppressor genes (Fig. 2C).

DNA Methylation Pattern of the ICR at the *Igf2/H19* Loci

COBRA was performed to detect the abnormal DNA methylation pattern of the ICR at the *Igf2*/*H19* loci in the thymus and the liver from $p53^{+/+}$, $p53^{+/-}$, and $p53^{-/-}$ mice at 7 weeks of age. Since the differential methylation at the region of the CTCF binding site 1 (nt. 1345–1392, GenBank accession no. U19619) and 2 (nt. 1592–1637) are more distinctive according to the parental alleles than the CTCF binding site 3 and 4, we analyzed the DNA methylation levels in the region containing the CTCF binding site 1 and 2 (Fig. 3A) [Reed et al., 2001]. The ClaI recognition site (ATCGAT) on the nucleotide 1389–1394 of the ICR at the end of the CTCF binding site 1 is abrogated after bisulfite conversion when the CpG sites are demethylated (Fig. 3A). Thus, the DNA methylation level of the CpG sites at the nucleotide 1391 could be evaluated by ClaI restriction enzyme (Fig. 3B). The thymus of $p53^{-/-}$ mice exhibited a considerable reduction of DNA methylation at the 1391 site, while the DNA methylation levels of the same site in the thymus of $p53^{+/+}$ and $p53^{+/-}$ mice were comparable with those in the liver (Fig. 3B). Lack of KpnI digest indicated the full bisulfite conversion. The *p53* deficiency did not affect the DNA methylation levels of the CpG sites in the liver.

To ascertain the influence of loss of *p53* on the comprehensive quality of the DNA methylation at the ICR, bisulfite sequencing of 1278–1749 under differential gene dosage of *p53* was performed in the thymus and the liver. Total of 16 CpG sites were analyzed (Fig. 3A). The overall percentages of the methylated CpGs in the thymus were 48.6% (451/928) in $p53^{+/+}$, 37.6% in $p53^{+/-}$ (349/928), and 9.6% (86/896) in $p53^{-/-}$ (Fig. 4A). The extents of the demethylation were increased by reduction of the *p53* dosage. The CpG dinucleotides in the thymus

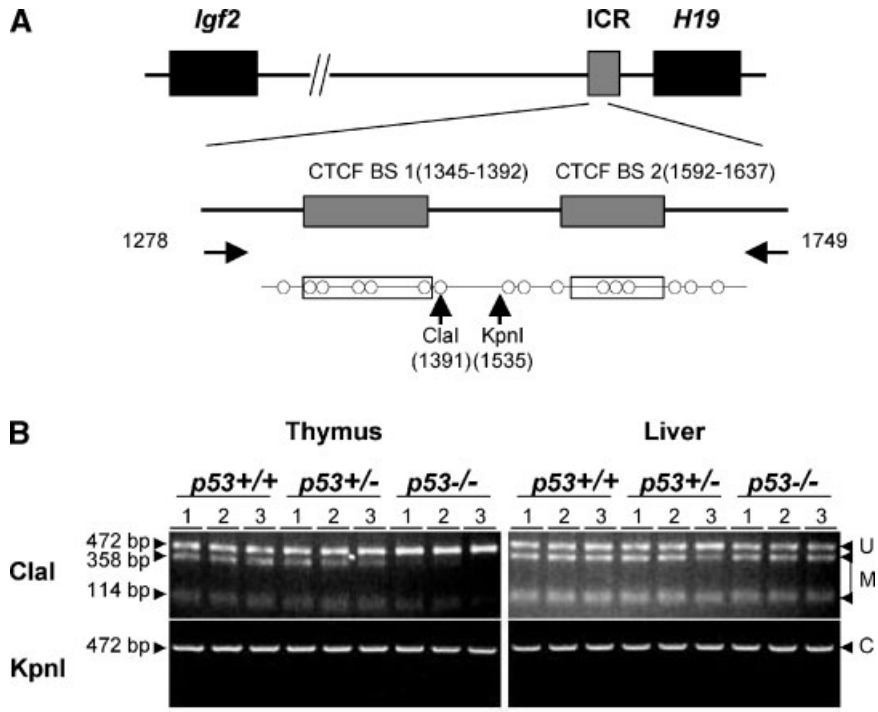

Fig. 3. The DNA methylation patterns of the ICR on the *Igf2/H19* loci in *p53*-deficient mice. **A**: Schematic map of the ICR containing the CTCF binding sites 1 and 2 (gray boxes) and the CpG sites (circles). Nucleotide-numbers according to GenBank U19619 sequence were indicated. Horizontal arrows indicate primers used for COBRA. The location of CpG sites are 1330, 1360, 1362, 1372, 1374, 1391, 1397, 1538, 1546, 1568, 1617, 1621, 1624, 1638, 1645, and 1658. The nucleotides at 1372 and 1374 were polymorphic sequences in C57BL/6J mice. Vertical arrows are the restriction enzyme sites used in COBRA. KpnI site (GGTACC) is located at 1531–1535. KpnI can cut only unconverted DNA but not fully converted DNA. Only fully converted PCR products were used. **B**: COBRA of the ICR on *Igf2/H19* loci. Digestion of the PCR products (472 bp) with ClaI yields 114 and 358 bp fragments when methylated. PCR products digested with KpnI were added as a bisulfite conversion control. To eliminate PCR bias, each of three samples from different individuals was repeatedly tested three times. U, unmethylated band; M, methylated bands; C, fully converted band.

were either methylated or unmethylated in $p53^{+/+}$ mice, presumably depending on the parental origin (Fig. 4A, $p53^{+/+}$ line 1). The DNA methylation pattern of the ICR was disturbed with a tendency of hypomethylation in the thymus of $p53^{+/-}$ and $p53^{-/-}$ (Fig. 4A, line 2 and line 3, respectively). No significant reduction of the CpG demethylation at the region was observed in the liver of $p53^{-/-}$ mice. The overall estimation of the methylated CpG sites in the liver was 47.5% (433/912) in $p53^{+/+}$, 37.7% (344/912) in $p53^{+/-}$, and 44.8% (409/912) in $p53^{-/-}$ (Fig. 4B). The quantity of the DNA methylation in the liver was slightly reduced in $p53^{+/-}$ mice as in the thymus. The CpG sites at nucleotide 1621 and 1624 within the CTCF binding site 2 seemed to be vulnerable to demethylation irrespective to *p53* dosage in the liver. The p53-dependent disruption of DNA methylation on the ICR of the *Igf2/H19* loci in the thymus suggests that the expression patterns of *Igf2* and *H19* could be affected in the thymus of *p53*-deficient mice.

Additional imprinted genes with well-defined DMR were investigated by COBRA [Lucifero et al., 2002]. The methylation of the DMRs of *Peg1* and *Peg3* could be evaluated by RsaI and Taq I, respectively. Bisulfite conversions of the DMRs were checked by HhaI digestion. The parental DNA methylation patterns of the DMRs at *Peg1* and *Peg3* were intact in the thymus and the liver of *p53*-deficient mice

Fig. 4. Bisulfite sequencing analysis of the ICR on the *Igf2/H19*. The region containing CTCF binding sites 1 and 2 has 16 CpG sites as illustrated in Figure 1A. Bisulfite sequencing data were performed with the PCR products obtained independently from three mice samples and plural independent clones. **A**: Thymus. **B**: Liver. Filled circles: Methylated CpG sites; open circles: Unmethylated CpG sites. Vertical arrows are the vulnerable CpG sites, 1621 and 1624, in the liver.

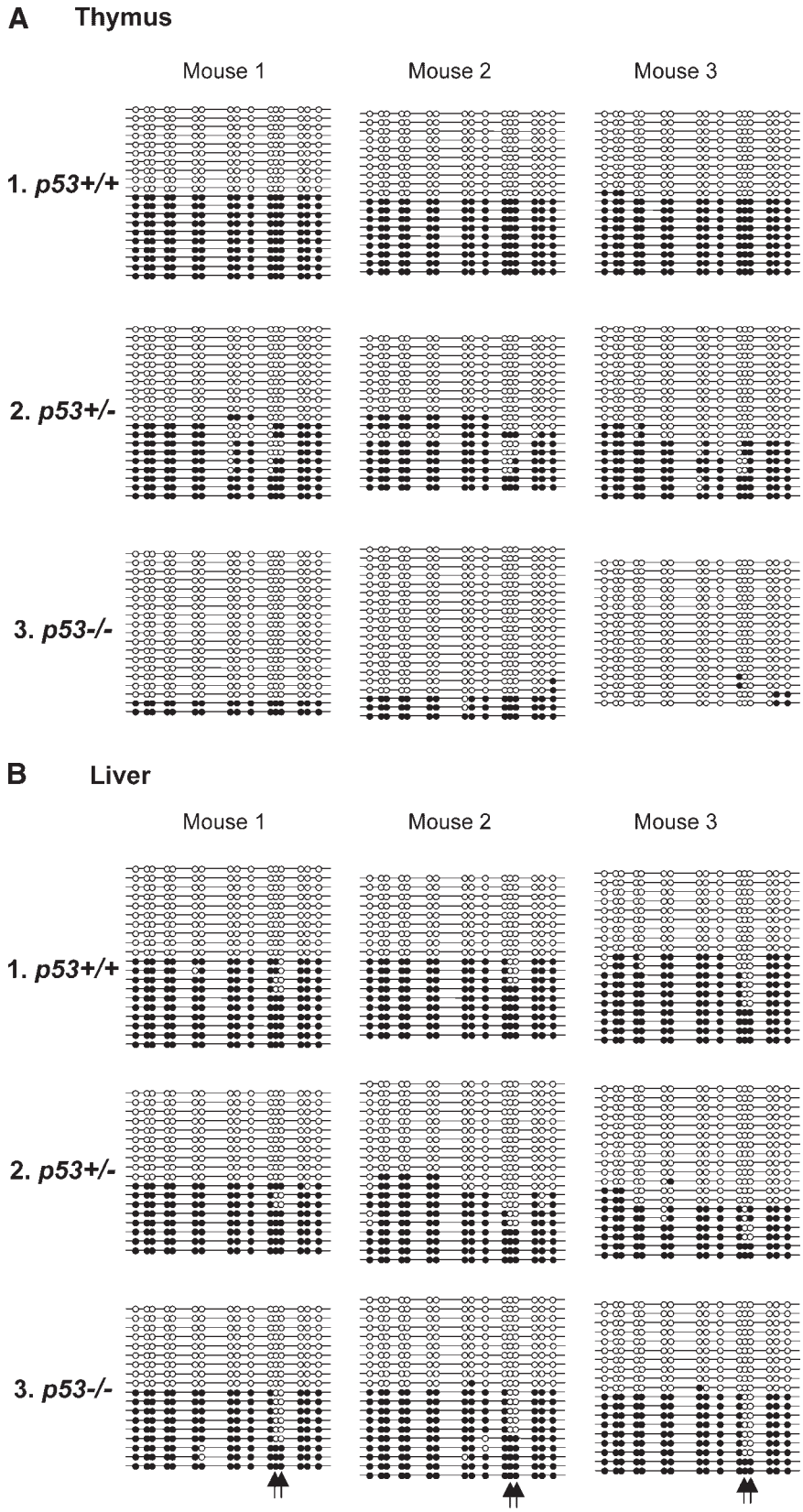
A Thymus
Mouse 1
Mouse 2
Mouse 3
1. p53+/+
2. p53+/-
3. p53-/-
B Liver
Mouse 1
Mouse 2
Mouse 3
1. p53+/+
2. p53+/-
3. p53-/-

Fig. 4.

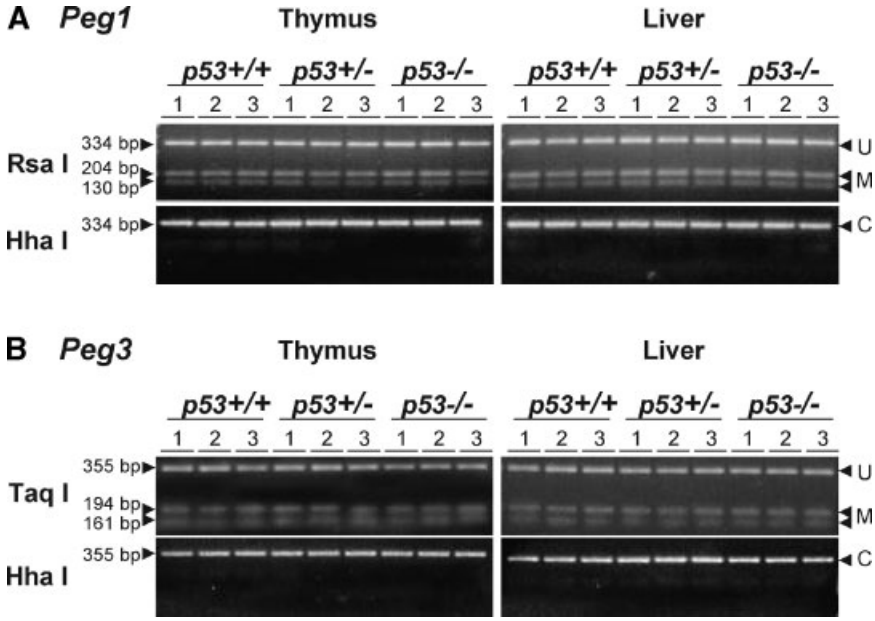

Fig. 5. The methylation patterns of *Peg1* and *Peg3*. **A**: COBRA of *Peg1*. RsaI digestion of the methylated DNA (334 bp) yield 204 and 130 bp fragments. Full bisulfite conversion was confirmed by HhaI digestion. U, unmethylated band; M, methylated bands; C, fully converted band. No changes of the methylation pattern were detected. **B**: COBRA of *Peg3*. TaqI digestion of the methylated DNA (355 bp) yield 194 and 161 bp fragments. Full bisulfite conversion was also confirmed by HhaI digestion. No changes of the methylation pattern were observed.

(Fig. 5A,B). The DNA methylation patterns in the maternally imprinted genes, *Peg1* and *Peg3*, did not seem to be influenced by the global methylation and/or the deregulated expression of DNA methyltransferases in *p53*-deficient mice.

Expression Profile of *Igf2* and *H19*

To correlate the disrupted DNA methylation pattern with the expressions of *Igf2* and *H19*, the expression levels of both genes were investigated under $p53^{+/-}$ and $p53^{-/-}$ conditions. *Igf2* expression was reduced in the thymus of $p53^{+/-}$ and $p53^{-/-}$ mice in a *p53* dose-dependent manner (Fig. 6A,B). The mRNA levels of *Igf2* in the thymus of $p53^{+/-}$ and $p53^{-/-}$ mice were 78.1 and 47.1%, respectively, relative to the wild type mice. The expression of *H19*, a reciprocally imprinted gene, showed an opposite pattern. *H19* mRNAs in the thymus of $p53^{+/-}$ and $p53^{-/-}$ mice were increased by 39.9 and 85.8%, respectively. Insignificant changes were observed in the liver, where a relatively consistent DNA methylation pattern of the ICR was maintained (Fig. 4B).

DISCUSSION

The expression of DNA methyltransferases was deregulated in *p53*-deficient mice before tumor development. The *p53* heterozygosity was sufficient to disrupt the regulation of DNA methyltransferases. Although the overexpression of DNA methyltransferases has been observed in many tumors, those epigenetic changes have been thought as outcome of tumorigenesis but not the direct effects of *p53* deficiency. Another evidence of the direct relationship between p53 and DNA methylation derived from a recent study demonstrates that *Dnmt1* is repressed by p53 binding on the exon 1 of *Dnmt1* in the absence of p53 activating stimuli [Peterson et al., 2003]. Our results provide a clue for understanding regulation of DNA methyltransferases by p53.

We have observed the hypomethylation of the CTCF binding sites 1 and 2 in the thymus under *p53* deficiency. The extent of the hypomethylation depends on *p53* gene dosage in the thymus, while the CTCF binding sites 1 and 2 were metastably methylated in the liver. It was previously shown that the CTCF insulator could bind to the unmethylated DNA and block the activation of *Igf2* by the *H19* enhancer [Bell and Felsenfeld, 2000; Hark et al., 2000]. The observed decrease of *Igf2* and the reciprocal increase of *H19* transcription in the thymus could be explained by the CTCF binding to the hypomethylated site 1 and 2 under *p53*-

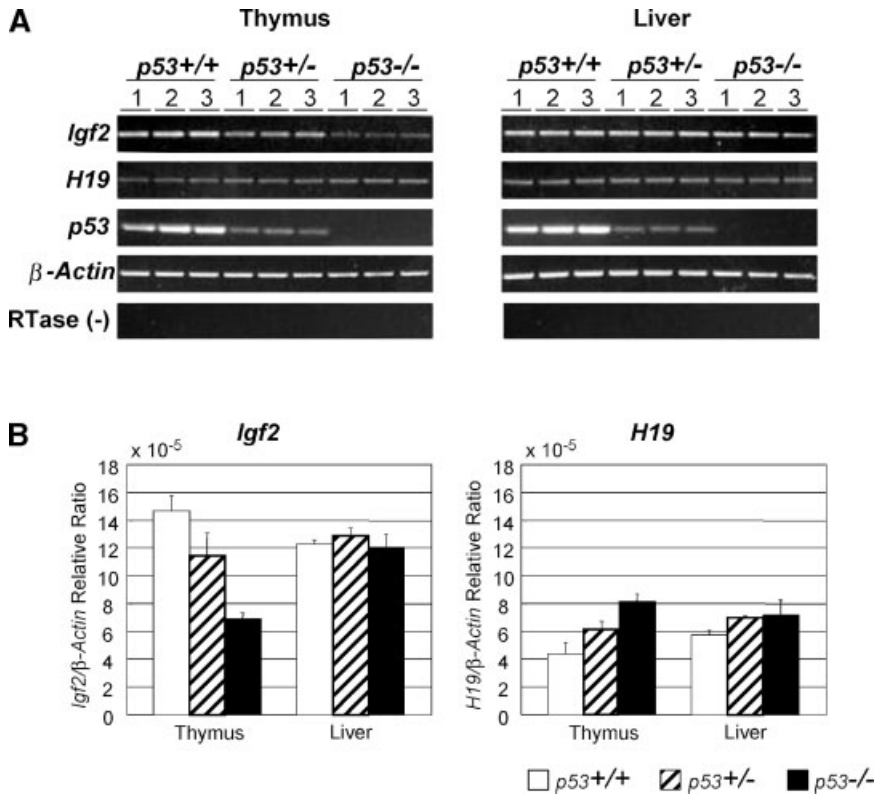

Fig. 6. The expression levels of *Igf2* and *H19*. **A**: Ethidium bromide staining of RT-PCR products. The RT-PCR cycle numbers of *Igf2*, *H19*, *p53*, and *β-Actin* were 35, 35, 25, and 22, respectively. The RT-PCR products from three independent wild type mice and *p53*-deficient mice were shown. RT (+) and RT (−) PCR with *β-Actin* primers was used as a control. No gender-dependent difference of mRNA quantities was detected. **B**: Quantitative real-time RT-PCR. The expression levels of *Igf2* and *H19* were quantitated by real-time RT-PCR with LightCycler using SYBR Green I dye. The relative amounts of the mRNAs were analyzed using Quantification program. The amount of the PCR products was normalized as percentage against the expression level of the control *β-Actin*.

deficiency. The metastable DNA methylation pattern in the liver reflects the consistent expression of *Igf2* and *H19* among $p53^{+/+}$, $p53^{+/-}$, and $p53^{-/-}$ mice. It is noted that the two CpGs of CTCF binding site 2 at 1621 and 1624 (arrows in Fig. 4B) were vulnerable to demethylation in the liver irrespective of *p53*-deficiency. It seems that individual cells in the liver are epigenetically heterogeneous.

The level of total 5-MeC was increased in *p53*-deficient mice. The increments of *Dnmt1* and *Dnmt3b* expression seemed to contribute to the global hypermethylation in *p53*-deficient mice. The increased expression of *Dnmt3a* in the liver of *p53*-deficient mice appears to represent the higher level of 5-MeC in the liver than the thymus. The observed global hypermethylation under *p53* deficiency contrasts with the genomic hypomethylation observed in most tumors [Jones and Baylin, 2002]. The maternally imprinted genes and the tumor suppressor genes examined in our studies evaded the shower of global methylation. The aberrant DNA methylation pattern of the ICR at the *Igf2*/*H19* loci suggests that the ICR may be governed by other epigenetic regulators in the thymus of $p53^{-/-}$ mice.

It can be concluded that p53 is required for the maintenance of DNA methylation patterns in vivo. The conclusion is supported by two main observations in this study; (1) *p53* deficiency results in the global hypermethylation through the overexpression of *Dnmt1* and *Dnmt3b* in vivo. (2) The ICR of the *Igf2*/*H19* loci in the thymus of $p53^{-/-}$ mice was hypomethylated before tumor development.

REFERENCES

Bell AC, Felsenfeld G. 2000. Methylation of a CTCF-dependent boundary controls imprinted expression of the *Igf2* gene. Nature 405:482–485.

Bourc'his D, Xu GL, Lin CS, Bollman B, Bestor TH. 2001. Dnmt3L and the establishment of maternal genomic imprints. Science 294:2536–2539.

Cui H, Niemitz EL, Ravenel JD, Onyango P, Brandenburg SA, Lobanenkov VV, Feinberg AP. 2001. Loss of imprinting of insulin-like growth factor-II in Wilms' tumor commonly involves altered methylation but not mutations of CTCF or its binding site. Cancer Res 61:4947–4950.

Cui H, Onyango P, Brandenburg S, Wu Y, Hsieh CL, Feinberg AP. 2002. Loss of imprinting in colorectal cancer linked to hypomethylation of H19 and IGF2. Cancer Res 62:6442–6446.

Cui H, Cruz-Correa M, Giardiello FM, Hutcheon DF, Kafonek DR, Brandenburg S, Wu Y, He X, Powe NR, Feinberg AP. 2003. Loss of IGF2 imprinting: A potential marker of colorectal cancer risk. Science 299:1753–1755.

Donehower LA, Harvey M, Slagle BL, McArthur MJ, Montgomery CA, Jr., Butel JS, Bradley A. 1992. Mice deficient for p53 are developmentally normal but susceptible to spontaneous tumours. Nature 356:215–221.

Ferguson-Smith AC, Cattanach BM, Barton SC, Beechey CV, Surani MA. 1991. Embryological and molecular investigations of parental imprinting on mouse chromosome 7. Nature 351:667–670.

Hark AT, Schoenherr CJ, Katz DJ, Ingram RS, Levorse JM, Tilghman SM. 2000. CTCF mediates methylation-sensitive enhancer-blocking activity at the H19/Igf2 locus. Nature 405:486–489.

Harvey M, McArthur MJ, Montgomery CA, Jr., Butel JS, Bradley A, Donehower LA. 1993. Spontaneous and carcinogen-induced tumorigenesis in p53-deficient mice. Nat Genet 5:225–229.

Hashimoto K, Azuma C, Koyama M, Ohashi K, Kamiura S, Nobunaga T, Kimura T, Tokugawa Y, Kanai T, Saji F. 1995. Loss of imprinting in choriocarcinoma. Nat Genet 9:109–110.

Hata K, Okano M, Lei H, Li E. 2002. Dnmt3L cooperates with the Dnmt3 family of de novo DNA methyltransferases to establish maternal imprints in mice. Development 129:1983–1993.

Hibi K, Nakamura H, Hirai A, Fujikake Y, Kasai Y, Akiyama S, Ito K, Takagi H. 1996. Loss of H19 imprinting in esophageal cancer. Cancer Res 56:480–482.

Jacks T, Remington L, Williams BO, Schmitt EM, Halachmi S, Bronson RT, Weinberg RA. 1994. Tumor spectrum analysis in p53-mutant mice. Curr Biol 4: 1–7.

Jones PA, Baylin SB. 2002. The fundamental role of epigenetic events in cancer. Nat Rev Genet 3:415–428.

Lucifero D, Mertineit C, Clarke HJ, Bestor TH, Trasler JM. 2002. Methylation dynamics of imprinted genes in mouse germ cells. Genomics 79:530–538.

Maniatis T, Fritsch EF, Sambrook J. 1982. Molecular cloning: A laboratory manual. Cold Spring Harbor, NY: Cold Spring Harbor Laboratory.

Peterson EJ, Bogler O, Taylor SM. 2003. p53-mediated repression of DNA methyltransferase 1 expression by specific DNA binding. Cancer Res 63:6579–6582.

Reed MR, Huang CF, Riggs AD, Mann JR. 2001. A complex duplication created by gene targeting at the imprinted H19 locus results in two classes of methylation and correlated Igf2 expression phenotypes. Genomics 74:186–196.

Robertson KD, Uzvolgyi E, Liang G, Talmadge C, Sumegi J, Gonzales FA, Jones PA. 1999. The human DNA methyltransferases (DNMTs) 1, 3a and 3b: Coordinate mRNA expression in normal tissues and overexpression in tumors. Nucleic Acids Res 27:2291–2298.

Srivastava S, Zou ZQ, Pirollo K, Blattner W, Chang EH. 1990. Germ-line transmission of a mutated p53 gene in a cancer-prone family with Li–Fraumeni syndrome. Nature 348:747–749.

Takeda S, Kondo M, Kumada T, Koshikawa T, Ueda R, Nishio M, Osada H, Suzuki H, Nagatake M, Washimi O, Takagi K, Takahashi T, Nakao A. 1996. Allelic-expression imbalance of the insulin-like growth factor 2 gene in hepatocellular carcinoma and underlying disease. Oncogene 12:1589–1592.

Tao L, Li Y, Kramer PM, Wang W, Pereira MA. 2004. Hypomethylation of DNA and the insulin-like growth factor-II gene in dichloroacetic and trichloroacetic acid-promoted mouse liver tumors. Toxicology 196:127–136.

Ulaner GA, Vu TH, Li T, Hu JF, Yao XM, Yang Y, Gorlick R, Meyers P, Healey J, Ladanyi M, Hoffman AR. 2003. Loss of imprinting of IGF2 and H19 in osteosarcoma is accompanied by reciprocal methylation changes of a CTCF-binding site. Hum Mol Genet 12:535–549.

Vu TH, Hoffman AR. 1994. Promoter-specific imprinting of the human insulin-like growth factor-II gene. Nature 371:714–717.

Weber M, Milligan L, Delalbre A, Antoine E, Brunel C, Cathala G, Forne T. 2001. Extensive tissue-specific variation of allelic methylation in the Igf2 gene during mouse fetal development: Relation to expression and imprinting. Mech Dev 101:133–141.

Xiong Z, Laird PW. 1997. COBRA: A sensitive and quantitative DNA methylation assay. Nucleic Acids Res 25: 2532–2534.